Electrostatic Levitation on Atmosphere-Less Planetary Bodies with Ionic-Liquid Ion Sources

Electrostatic Levitation on Atmosphere-Less Planetary Bodies with Ionic-Liquid Ion Sources

Oliver Jia-Richards[1], Sebastian K. Hampl[2] and Paulo C. Lozano[3]
Massachusetts Institute of Technology, Cambridge, Massachusetts, 02139

This paper presents an initial feasibility study on the use of ionic-liquid ion sources for electrostatic actuation on atmosphere-less planetary bodies. The natural surface charging of atmosphere-less planetary bodies has been studied as the cause of the transport of regolith across the surface and for electrostatic levitation of a spacecraft in proximity to small asteroids. The low magnitude of the natural surface electric field (order 10 V/m) severely limits the capability of a vehicle to leverage electrostatic levitation as its maneuvering strategy, particularly on large planetary bodies such as the Moon. Ionic-liquid ion sources are considered as an actuator for charging of both the vehicle as well as the local surface of the planetary body. By irradiating the surface with ions, the surface electric field can be increased far beyond its natural value and could enable electrostatic levitation on planetary bodies as large as the Moon with current technology. A low-fidelity analytical model of the charging process is developed in order to estimate requirements on the local surface charge density and limitations on the vehicle's levitation height and translational speed. Experiments are conducted in a laboratory environment to demonstrate the feasibility of using ionic-liquid ion sources for combined vehicle and surface charging by creating a 1 mN electrostatic force through charge transport while requiring only 0.2 mW of input power. These experiments are in reasonable agreement with the low-fidelity model that describes the fundamental physics of this concept.

---

[1] Doctoral Candidate, Department of Aeronautics and Astronautics, oliverjr@mit.edu, Student Member AIAA
[2] Visiting Student, Department of Aeronautics and Astronautics, sebastian.hampl@tum.de
[3] Professor, Department of Aeronautics and Astronautics, plozano@mit.edu, Associate Fellow AIAA

Nomenclature

A_s = surface charged area [m^2]

A_v = vehicle charged area [m^2]

C_v = vehicle capacitance [F]

d = displacement of the tungsten rod [m]

E = electric field [N/m]

E_s = surface electric field [N/m]

E_v = vehicle electric field [N/m]

F = force [N]

F_a = attractive force [N]

F_r = repulsive force [N]

g = gravitational acceleration [$\mathrm{m/s}^2$]

h = height [m]

h^* = maximum operational height [m]

$\bar{h}$ = normalized height [m]

k = spring constant [N/m]

l = distance between emitter tip and extractor grid [m]

m_v = vehicle mass [kg]

q_s = surface charge [C]

q_v = vehicle charge [C]

r_s = radius of the charged area on the surface [m]

r_v = vehicle radius [m]

R = planetary body radius [m]

R_c = radius of curvature [m]

t = charging time [s]

u = characteristic speed [$\mathrm{m/s}^2$]

V_th = thruster/source potential [V]

V_start = starting potential [V]

γ = surface tension [N/m]

δ = reduction factor [-]

ρ = planetary body mass density [kg/m^3]

σ_s = surface charge density of the surface [C/m^2]

σ_v = surface charge density of the vehicle [C/m^2]

I. Introduction

The interaction between surfaces of atmosphere-less planetary bodies, such as the Moon and asteroids, and the surrounding plasma and radiation environment can induce surface charging. Due to the low plasma density, this surface charging allows for electric fields extending up to tens of meters away from the surface. Analysis of the data from the Suprathermal Ion Detector Experiment on the Apollo missions [1] and the Electron Reflectometer from the Lunar Prospector mission [2] both confirm the presence of surface charging on the Moon and resulting electric fields on the order of 10 V/m. This electric field is large enough to levitate the regolith on the surface of the Moon, and the Surveyor landers observed $\sim$10 μm grains of dust levitating $\sim$1 m above the surface [3].

Although these experiments were conducted on the Moon, surface charging will occur on any planetary body without a sufficiently strong charge-dissipation mechanism such as an atmosphere or internal charge dissipation. Theoretical calculations predict surface electric fields on the order of 10-20 V/m on the Sun-facing surface of asteroids in the main asteroid belt [4]. It is believed that this surface charging is responsible for the transport of dust on atmosphere-less planetary bodies, which could explain phenomena such as the unusually smooth surface of Atlas [5], "ponds" of dust on Eros as seen by the NEAR Shoemaker mission [6], degradation of optical devices on the Moon [7], porosity on the surfaces of asteroids [8], and emission and redistribution of particles on the comet Churyumov-Gerasimenko [9, 10].

To support this theory, laboratory experiments have been able to demonstrate the electrostatic transportation of dust particles on dusty surfaces under ultraviolet illumination or exposure to plasmas. Dust is observed to shed from a conductive sphere when exposed only to a plasma [11], but required a plasma and electron beam when the dust was placed on an insulating surface [12, 13].

Other experiments attempted to quantify the charging on dust particles when exposed to a plasma [14]. In experiments more representative of asteroid surfaces, shadow boundaries, like what might be seen at the terminator between the day and night sides of an asteroid, were found to increase dust transport [15], and the use of ultraviolet illumination in combination with an ambient plasma was found to induce dust charging and transport [16].

From the observation of the levitation of dust particles, an electrostatic glider concept was proposed in order to utilize this natural surface charging to provide maneuverability around a small asteroid [17]. The electrostatic glider deploys Mylar wings in order to increase its capacitance such that electrostatic levitation can be achieved. However, the set of planetary bodies that can be explored with such a concept is limited to small asteroids due to the relatively low surface electric field. To resolve the issues associated with low natural surface charging and enable electrostatic levitation on larger planetary bodies, this work proposes the use of microfabricated ionic-liquid ion sources to charge the spacecraft body as well as to artificially increase the local surface charge of the planetary body's surface beyond the natural limit.

Ionic-liquid ion sources are devices that produce beams of ions from the surface of a room-temperature molten salt, or ionic liquid. Depending on the polarity of the applied field, ions could be positively or negatively charged. These ion sources have been mainly developed as extremely compact electrospray thrusters for propelling small satellites in space and several devices manufactured using microfabrication techniques have been proposed [18–21]. Electrospray thrusters could be operated in pairs in a bipolar configuration in order to maintain a near-neutral vehicle charge and eliminate the need for a neutralization cathode [22]. By de-activating a thruster in the pair, a single thruster can be used to charge the vehicle close to the potential applied to the thruster.

To artificially increase the charging of the planetary body's surface, an ionic-liquid ion source could be used to irradiate the surface with ions and increase the local surface charging. Such a strategy would allow for surface electric fields well in excess of the natural $\sim$10 V/m. In this concept one ion source ejects negative ions upward from the vehicle to charge it positively, while a second fires positive ions downward into the surface in order to charge the local surface positively and increase the local electric field. Additional sources, in the form of electrospray thrusters, can be included

to provide translational maneuverability. Since electrospray thrusters are solid-state devices, such a system could allow for a vehicle that can achieve levitation and translational movement across a planetary body's surface with no moving parts. In addition, as the vehicle is levitating, it has no physical contact with the planetary body's surface, potentially allowing it to more easily explore uneven surfaces relative to traditional wheeled or hopping vehicles.

This work is an initial feasibility study on the use of ionic-liquid ion sources for electrostatic actuation for a small vehicle around atmosphere-less planetary bodies. An important distinction between the concept developed here and that of Ref. [17], is that that the vehicle is assumed to be deployed directly on the surface of the planetary body, analogous to a rover, rather than in proximity operations. A low-fidelity analytical model of the charging process is developed in order to estimate requirements on vehicle and surface charging for levitation on various planetary bodies along with theoretical bounds on translational velocity and levitation height. In addition, laboratory experiments demonstrate the capability for ionic-liquid ion sources to induce surface charging on a metal plate and artificially create a local surface electric field. Measurements of the resulting electrostatic force show that the experimental results are in reasonable agreement with the low-fidelity model that describes the fundamental physics of this concept.

II. Vehicle Charging

Vehicle charging is caused by a net current flow in or out of the vehicle. For spacecraft, this net current is often from an imbalance in particle flux between electrons and ions in the surrounding plasma environment which will cause the spacecraft to charge negatively, or from photoelectron emission which will cause the spacecraft to charge slightly positive. However, the use of electric propulsion devices introduces a new current in the form of emitted ions. Most electric propulsion devices eject positive ions at currents much greater than that of the particle flux or photoelectron emission, causing the parent spacecraft to charge negatively. If this negative charging is left unchecked, the spacecraft will charge such that all of the emitted ions are attracted back to the spacecraft's body and no thrust will be produced.

In order to prevent spacecraft charging, neutralizers are used to both limit the net current flow

out of the spacecraft and the neutralize the thruster plume. Since ionic-liquid electrospray thrusters can emit both positive and negative ions, they can act as their own neutralizer. Typical operation involves bipolar operation of pairs of thrusters where one emits positive ions and the other emits negative ions. Ideally, the two thrusters would emit equal currents. However, small differences in thruster performance mean that some level of spacecraft charging is unavoidable. Fortunately, the presence of low-energy ions in electrospray thruster plumes due to fragmentation processes [23] limits the subsequent spacecraft charging [22], and allows for operation of electrospray thrusters in a bipolar configuration without the need for an external neutralizer.

In the concept explored in this work, vehicle charging is intentionally induced by the use of a single ionic-liquid ion source emitting either positive or negative ions. As the vehicle charges, lower-energy ions will begin to return to the vehicle, lowering the overall net current. However, due to the lack of any neutralization scheme, the vehicle will charge close to the potential of the ions with the highest energy. Figure 1 shows a typical energy distribution of an ionic-liquid ion source plume measured with a retarding potential analyzer. Current, normalized by the total current in the beam, is measured versus retarding potential, normalized by the applied source potential. As the retarding potential increases beyond the energy of certain ions in the plume, those ions will no longer be able to reach the instrument and therefore the measured current will drop. Distinct steps can be seen in the plot due to low-energy ions created from fragmentation processes external to the thruster. However, almost half of the ions in the beam have energy close to the source potential, meaning that the vehicle will charge close to the source potential in free space. Additionally, even with the presence of external plasma and photoelectron currents, the output current of an electrospray thruster is approximately 150 μA [21] which is several orders of magnitude greater than the predicted $\sim$100 nA of photoelectron current for a small vehicle with a diameter of 10 cm [24] which in turn is large relative to the predicted plasma current on a body such as the Moon [25]. As such, equilibrium in the presence of external plasma and photoelectron currents will still require that the vast majority of the ion beam return to the vehicle implying that the vehicle will still charge close to the source potential.

Assuming the vehicle charges close to the source potential, then the charge on the vehicle, q_{v},

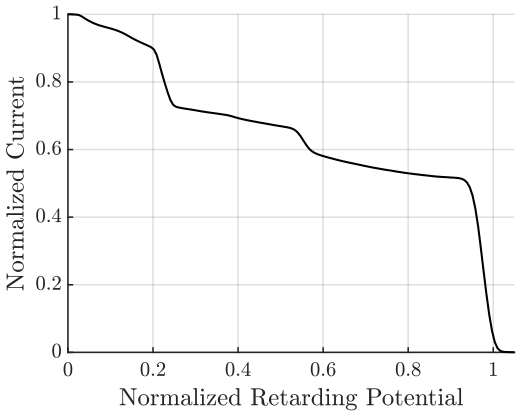

Fig. 1 Typical energy distribution from an electrospray thruster plume [23].

can be calculated from

$$q_{\mathrm{v}} = C_{\mathrm{v}} V_{\mathrm{th}} \tag{1}$$

where C_{v} is the capacitance of the vehicle relative to infinity and V_{th} is the source potential. The capacitance of a small vehicle with characteristic dimension of 10 cm is on the order of 10 pF. It is assumed here that the rover is operating directly on the surface of the planetary body and therefore cannot deploy wings in order to increase its capacitance as is considered in Ref. [17]. Typical source potentials of microfabricated electrospray thrusters are on the order of 1 kV, however the beam could be further accelerated through the use of additional electrodes in order to increase this value to the order of 10 kV or more. Therefore, the expected charge of the vehicle is on the order of 100 nC. Electrostatic levitation can be achieved if the electrostatic force is equal to the weight of the vehicle

$$m_{\mathrm{v}} g = q_{\mathrm{v}} E \tag{2}$$

where m_{v} is the mass of the vehicle, g is the local gravitational acceleration, and E is the local electric field. For an assumed vehicle mass of around 1 kg and local electric field of 10 V/m, the local gravitational acceleration needs to be on the order of 1 μm/s^2.

Such a small gravitational acceleration is restricted to very small planetary bodies. Assuming a spherical planetary body of radius R and uniform mass density ρ, the gravitational acceleration

Table 1 Vehicle and planetary body parameters.

Parameter	Value
Vehicle mass	1 kg
Vehicle dimension	10 cm
Thruster potential	10 kV
Surface electric field	10 V/m
Planetary body mass density	3.34 g/cm^3

on the surface is given by

$$g = \frac{4}{3} G \pi \rho R \tag{3}$$

where G is the universal gravitational constant. Assuming a mass density of 3.34 g/cm^3, the average mass density of the Moon, the approximate order of magnitude for the largest planetary body where levitation could be achieved from natural surface charging on the Sun-facing surface is one meter. Levitation on larger planetary bodies could be achieved on the night side or at the terminator due to the greater electric field. However, operation on the night side would be heavily limited by the ability for the vehicle to generate power and operation at the terminator restricts the area of the planetary body the vehicle can explore.

Figure 2 shows an estimate of the maximum planetary body radius on which levitation could be achieved versus source potential for the same vehicle and planetary body parameters, summarized in Table 1. A source potential of 1 MV would be required in order to achieve levitation on a 130 m planetary body. Even for planetary bodies with significant porosity such that their mass density is closer to 1 g/cm^3 such as the asteroid 2011 MD [26], the required source potential for levitation will still be of the same order. These magnitudes would be very challenging to achieve, especially on a compact vehicle.

III. Surface Charging

In order to enable electrostatic levitation for such a small vehicle without requiring impractically high thruster potentials, the local surface electric field of the planetary body would need to be artificially increased. Ionic-liquid ion sources could be used to irradiate the surface directly below

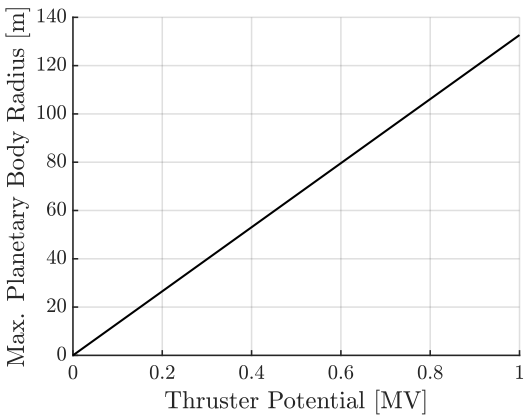

Fig. 2 Maximum planetary body radius where levitation could be achieved from natural surface charging with a 1 kg, 10 cm vehicle versus thruster potential. Planetary body is assumed to be spherical with a uniform mass density of 3.34 g/cm^3 and surface electric field of 10 V/m.

the vehicle with ions to charge it, thereby modifying the magnitude of the local electric field. Initially, with the vehicle at rest on the planetary body's surface, ions can be emitted from the vehicle directly into the surface thereby charging both the vehicle and the local surface. As with the vehicle charging analysis, the current of an electrospray thruster is expected to dominate any external currents. Therefore, plasma and photoelectron currents are neglected during this analysis.

Since the vehicle starts on the surface of the planetary body, it is assumed that all the emitted ions either reach the surface or return to the vehicle. In this case, the charge of the vehicle will be equal but opposite to the charge on the surface

$$-q_{\mathrm{v}} = q_{\mathrm{s}} = q \tag{4}$$

where q_{s} is the charge on the surface. The surface charge densities on the vehicle and surface are therefore

$$\sigma_{\mathrm{v}} = -\frac{q}{A_{\mathrm{v}}} \quad \text{and} \quad \sigma_{\mathrm{s}} = \frac{q}{A_{\mathrm{s}}} \tag{5}$$

where A_{v} and A_{s} are the surface area of the vehicle and the charged surface respectively. The surface area of the vehicle will typically be the surface area of the vehicle's body while the surface area of the charged surface will depend on what area is irradiated by the ion plume. This analysis assumes

that the charge is evenly distributed on the vehicle's body. In reality, the charge distribution will be uneven and depend on the shape of the vehicle. Since this effect will be unique to different vehicles, it is neglected here.

Approximating the distance between the vehicle and the surface as small with respect to extent of A_v and A_s, and the geometry of the vehicle and surface charge as that of a flat plate, then the magnitude of the electric field between the vehicle and surface is approximately

$$E \approx \frac{q}{2\epsilon_0 A_\mathrm{s}} + \frac{q}{2\epsilon_0 A_\mathrm{v}} \tag{6}$$

where ϵ_0 is the permittivity of free space. The vehicle and surface will continue to charge until the potential difference between the vehicle and surface is equal to the thruster potential

$$Eh = \frac{qh}{2\epsilon_0}\left(\frac{1}{A_\mathrm{s}} + \frac{1}{A_\mathrm{v}}\right) = V_\mathrm{th} \tag{7}$$

where h is the initial distance between the vehicle and surface. Once this condition is met, no ions will be able to reach the surface and will all return back to the vehicle. The resulting equilibrium charge is

$$q = \frac{2\epsilon_0 V_\mathrm{th}}{h}\left(\frac{A_\mathrm{s}A_\mathrm{v}}{A_\mathrm{s}+A_\mathrm{v}}\right) \tag{8}$$

which produces a local electric field from the surface of

$$E_\mathrm{s} = \delta\frac{q}{2\epsilon_0 A_\mathrm{s}} = \delta\frac{V_\mathrm{th}}{h}\left(\frac{A_\mathrm{v}}{A_\mathrm{s}+A_\mathrm{v}}\right) \tag{9}$$

where $\delta \in (0,1)$ accounts for a reduction in the electric field due to three dimensional effects. Approximating the local surface charging as a disk then the electric field along its center axis is given by

$$E_\mathrm{s}(h) = E_{\mathrm{s},0}\left(1 - \frac{h}{\sqrt{h^2 + r_\mathrm{s}^2}}\right) \tag{10}$$

where $E_{\mathrm{s},0}$ is the electric field of an infinite flat plate and r_s is the radius of the charged area. The reduction factor, δ, can then be estimated as

$$\delta(h) = 1 - \frac{h}{\sqrt{h^2 + r_\mathrm{s}^2}} \tag{11}$$

which gives an electric field at the height of the vehicle of

$$E_{\mathrm{s}}(h) = \delta(h)\frac{V_{\mathrm{th}}}{h}\left(\frac{A_{\mathrm{v}}}{A_{\mathrm{s}}+A_{\mathrm{v}}}\right) \tag{12}$$

and an attractive electrostatic force of

$$F_{\mathrm{a}} = qE_{\mathrm{s}}(h) = \delta(h)\frac{2\epsilon_0 V_{\mathrm{th}}^2}{h^2}\left(\frac{A_{\mathrm{s}}A_{\mathrm{v}}^2}{\left(A_{\mathrm{s}}+A_{\mathrm{v}}\right)^2}\right) \tag{13}$$

This electrostatic force could be used to anchor the vehicle to the surface. Using a vehicle with parameters given by Table 1, approximating the local surface charging to have the same area as the area of the vehicle such that $r_{\mathrm{s}} = 10$ cm, and assuming a distance between the vehicle and surface of 2 cm, then the electrostatic force is approximately 56 mN which is sufficient to anchor a small ($\sim$1 kg) spacecraft to fast-rotating asteroids such as 1999 TY2, 1999 SF10, and 1998 WB2 [27].

In order to achieve levitation, the vehicle needs to be charged to the same polarity as the surface. This can be achieved by emitting ions away from the surface, thereby charging the vehicle but not affecting the surface charge. The magnitude of the vehicle charge will be given by Eq. 1 which results in a repulsive electrostatic force of

$$F_{\mathrm{r}} = C_{\mathrm{v}}V_{\mathrm{th}}E_{\mathrm{s}}(h) = \delta(h)\frac{C_{\mathrm{v}}V_{\mathrm{th}}^2}{h}\left(\frac{A_{\mathrm{v}}}{A_{\mathrm{s}}+A_{\mathrm{v}}}\right) \tag{14}$$

For levitation, the electrostatic force needs to be sufficient to counter the local gravitational force

$$F_{\mathrm{r}} = \delta(h)\frac{C_{\mathrm{v}}V_{\mathrm{th}}^2}{h}\left(\frac{A_{\mathrm{v}}}{A_{\mathrm{s}}+A_{\mathrm{v}}}\right) \geq m_{\mathrm{v}}g \tag{15}$$

which can be solved for the required source potential

$$V_{\mathrm{th}} = \sqrt{\frac{m_{\mathrm{v}}gh}{C_{\mathrm{v}}\delta(h)}\left(\frac{A_{\mathrm{s}}+A_{\mathrm{v}}}{A_{\mathrm{v}}}\right)} \tag{16}$$

Figure 3 shows the required source potential in order to achieve levitation versus surface gravitational acceleration for vehicle parameters given by Table 1, a distance between the vehicle and surface of 2 cm, and assuming that the radius of the surface charging is equal to the radius of the vehicle. The thruster potential is shown both for the case where the natural surface charging is used and for the case where the surface charging is artificially increased through ion bombardment. Focusing on the Moon, when using only the natural surface charging a thruster potential of over 10 GV would

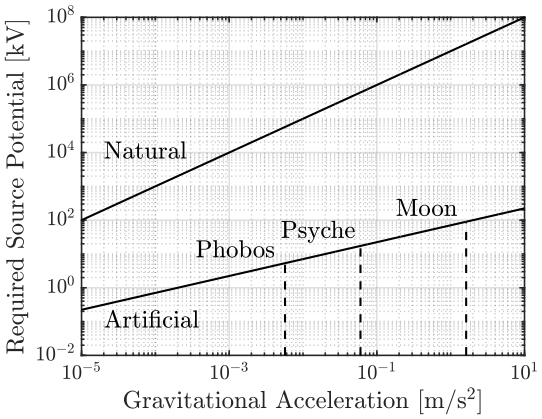

Fig. 3 Required source potential in order to achieve levitation versus surface gravitational acceleration when using just the natural surface charging and when artificially increasing the natural surface charging through ion bombardment. Data is shown for a 1 kg, 10 cm vehicle with an initial vehicle-to-surface distance of 2 cm.

be required to achieve levitation. If the surface charging is artificially increased, levitation could be achieved with a thruster potential of 100 kV, a potential that is feasible with current technology.

Once levitation has been achieved, the vehicle can modify its charge in order to control its altitude. However, it is likely that the vehicle will also have to maintain the local surface charging in order to counter any slow charge dissipation to the surrounding plasma environment or into the bulk of the planetary body. As such, the maximum operational levitation height of the vehicle will be limited. If the vehicle levitates too high, then the potential difference between the vehicle and the surface will be larger than the source potential and ions will not be able to reach the surface. In addition, as the vehicle traverses across the surface it will have to charge any new, uncharged, surface it encounters. Therefore, the translational speed of the vehicle will be limited by the time-scale at which the local surface can be charged to the required surface charge density for levitation.

A. Levitation Height

The local surface electric field which enables vehicle levitation also repels ions used to charge the surface. For a given maximum ion energy, set by the thruster potential, if the levitation height is too large then ions will be unable to reach the surface, preventing the required surface charging from being maintained in the presence of plasma currents and photoelectron emission. While the

vehicle is not strictly unable to levitate beyond this height (it could momentarily increase its own body charge in order to levitate higher) it would lose the ability to control the local surface charge. As such, it is likely that during operations, the vehicle will maintain a levitation height such that it can control the local surface charge.

The electric field between the vehicle and the surface is the superposition of the electric field from the vehicle and the electric field from the surface. The magnitude of the surface electric field required for levitation is given by

$$E_{\mathrm{s}} = \frac{m_{\mathrm{v}} g}{C_{\mathrm{v}} V_{\mathrm{th}}} \tag{17}$$

Approximating the vehicle as a disk with uniform charge distribution on the top and bottom surfaces, then its surface charge density is given by

$$\sigma_{\mathrm{v}} = \frac{C_{\mathrm{v}} V_{\mathrm{th}}}{2\pi r_{\mathrm{v}}^2} \tag{18}$$

where r_{v} is the radius of the vehicle. This surface charge density produces an electric field of

$$E_{\mathrm{v}} = \frac{\sigma_{\mathrm{v}}}{\epsilon_0} = \frac{C_{\mathrm{v}} V_{\mathrm{th}}}{2\epsilon_0 \pi r_{\mathrm{v}}^2} \tag{19}$$

In order for ions to reach the surface, the potential difference between the vehicle and the surface needs to be less than the highest energy ions emitted by the thruster. Ions used to charge the surface will be repelled by the surface and the vehicle. However, repulsion away from the vehicle aids in "pushing" the ions towards the surface. Therefore, the height of the vehicle at which ions, accelerated through the thruster potential, V_{th}, will no longer be able to reach the surface is given by

$$h^* \approx \frac{V_{\mathrm{th}}}{E_{\mathrm{s}} - E_{\mathrm{v}}} \tag{20}$$

For cases in which $E_{\mathrm{s}} \leq E_{\mathrm{v}}$ there is no limitation on the levitation height. However, this analysis assumes that the levitation height is small relative to the extent of the local surface charging and the characteristic dimension of the vehicle, and will be invalid for large levitation heights due to three dimensional effects of the surface electric field. Substituting Eqs. 17 and 19 into Eq. 20 gives

$$h^* \approx \frac{2\pi\epsilon_0 r_{\mathrm{v}}^2 C_{\mathrm{v}} V_{\mathrm{th}}^2}{2\pi\epsilon_0 m_{\mathrm{v}} g r_{\mathrm{v}}^2 - C_{\mathrm{v}}^2 V_{\mathrm{th}}^2} \tag{21}$$

Approximating the capacitance of the vehicle as that of a finite disk with uniform charge distribution, then

$$C_{\mathrm{v}} \approx 2\pi\epsilon_0 r_{\mathrm{v}} \tag{22}$$

which allows the maximum operational levitation height to be reduced to

$$h^* \approx \frac{2\pi\epsilon_0 r_{\mathrm{v}} V_{\mathrm{th}}^2}{m_{\mathrm{v}} g - 2\pi\epsilon_0 V_{\mathrm{th}}^2} \tag{23}$$

and leads to a non-dimensional maximum levitation height

$$\bar{h} = \frac{h^*}{r_{\mathrm{v}}} \approx \frac{2\pi\epsilon_0 V_{\mathrm{th}}^2}{m_{\mathrm{v}} g - 2\pi\epsilon_0 V_{\mathrm{th}}^2} \tag{24}$$

normalized by the vehicle characteristic dimension.

Figure 4 shows the non-dimensional maximum levitation height versus surface gravitational acceleration for vehicle parameters given by Table 1 including a thruster potential of 50 kV. For 10 kV, the normalized levitation height for planetary bodies with surface gravitational acceleration similar to Psyche is around 0.1, potentially enabling the vehicle to traverse across the surface. If the thruster potential is increased to 50 kV, similar levitation heights could be maintained on planetary bodies as large as the Moon. More detailed analysis of the electric field between the vehicle and the surface is required to fully capture three dimensional effects. However, per this initial analysis, maintaining electrostatic levitation with ionic-liquid electrospray thrusters should be achievable with current technology.

Plasma shielding due to the surrounding plasma environment will also limit the levitation height of the vehicle. However, theoretical predictions of the smallest Debye length, due to photoemission on the Sun-facing surface of a planetary body, are 50+ cm [4]. Therefore, for levitation heights of a few tens of cm, the vehicle will be operating within a Debye length of the surface and the surface electric field should not be significantly attenuated. In addition, the strong surface charging created by ion bombardment should serve to extend the plasma sheath.

B. Translational Speed

As the vehicle traverses across the planetary body surface, any new, uncharged, surface it encounters needs to be charged to the required surface charge density for levitation. If the required

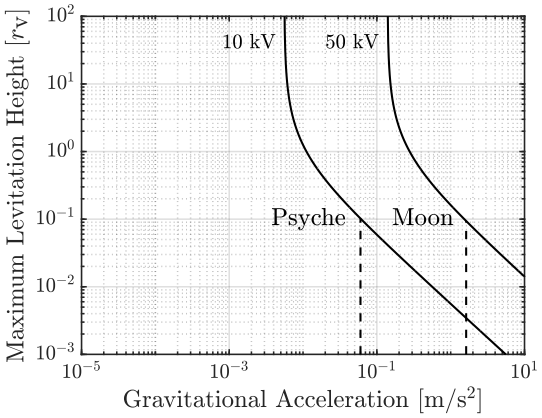

Fig. 4 Maximum levitation height normalized by the vehicle's characteristic dimension at which the local surface charge can be controlled versus surface gravitational acceleration for source potentials of 10 kV and 50 kV and assumed vehicle mass of 1 kg.

surface charge density is too high, then the vehicle's translational speed will be limited in order to ensure proper surface charging is achieved. Assuming that all the current, I, emitted by a thruster goes into charging the surface below the vehicle, then the time required to achieve a local charge density is given by

$$t = \frac{\pi r_s^2 \sigma_s}{I} = \frac{2\pi\epsilon_0 r_s^2 E_s}{I} \tag{25}$$

Typical ionic-liquid electrospray thruster currents are 100-200 μA [21]. Figure 5 shows the surface charging time if the thruster used to charge the surface is operated at 100 μA versus surface gravitational acceleration for vehicle parameters given by Table 1. Even for planetary bodies as large as the Moon, the required surface charging time is less than 100 ms. This means that the vehicle will not be significantly limited in its ability to move across the surface.

The characteristic speed that the vehicle will be able to move across the surface while maintaining the required surface charge density for levitation scales with

$$u = \frac{r_s}{t} \tag{26}$$

For the Moon, the characteristic speed is approximately 1.2 m/s, which is comparable to that of the crewed Lunar Roving Vehicle [28] and two orders of magnitude greater than that of the Lunokhood rovers [29].

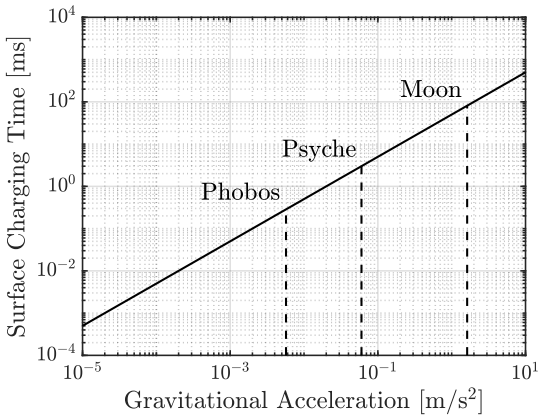

Fig. 5 Required charging time for vehicle levitation versus surface gravitational acceleration. A charging current of 100 μA is assumed for a 1 kg, 10 cm vehicle with capacitance equal to that of a finite disk with uniform charge distribution.

The assumption that all of the emitted current will go into charging the planetary body surface is the main unknown for such a concept. The surface charging will depend not only on the ion flux from the ion source, but also on the properties of the surface materials, which can vary between planetary bodies and control secondary charge emission and charge dissipation. Nevertheless, even if only 10% of the emitted current goes into charging the surface, the characteristic speed of the vehicle on the Moon will be 0.12 m/s and still allow for efficient surface exploration comparable to that of wheeled rovers.

Also of importance is the time required to charge the vehicle body. Assuming that 200 μA of current is emitted away from the planetary surface, so as to charge the vehicle but not the planetary surface, then the net current leaving the vehicle, taking into account the 100 μA of current used to charge the surface, is 100 μA. The self-capacitance of the vehicle is approximately 10 pF giving a theoretical charging rate of 10 MV/s. Therefore, the vehicle body can be charged to the required 10 kV potential in $\sim$50 μs, faster than the time required to charge the surface until objects smaller than Phobos ($\leq$ 10 km) are considered. However, unlike surface charging, charging of the vehicle body only needs to be done once, assuming minimal charge loss, as the vehicle traverses across the surface. Both the time to charge the vehicle body and time to charge the surface are small relative to any time scales desired for surface maneuverability meaning that the charging time will not be

Table 2 Summary of derived parameters for a 1 kg, 10 cm rover with capacitance equal to that of a finite disk with uniform charge distribution. It is assumed that a source current of 100 μA is used to charge the planetary body surface.

Parameter	Psyche (0.06 m/s^2)	Moon (1.62 m/s^2)
Required source potential	10 kV	50 kV
Maximum levitation height	1 cm	1 cm
Surface charging time	3 ms	81 ms
Characteristic vehicle speed	33 m/s	1.25 m/s

the limiting factor in the ability for the vehicle to traverse across the surface.

Table 2 summarizes the vehicle characteristic speed as well as previously derived parameters for a 1 kg, 10 cm rover operating on a planetary bodies similar to Psyche and the Moon, with surface gravitational accelerations of 0.06 m/s^2 and 1.62 m/s^2 respectively. The required source potential is taken to be the minimum source potential at which a rover would be able to levitate to 0.1 its characteristic dimension, 1 cm in this case, under the assumption that the charge distribution on the vehicle can be approximated as that of a uniformly charged flat disk and that the extent of the surface charging is much larger than the characteristic dimension of the vehicle. The vehicle could levitate to greater heights with larger source potentials, but more detailed analysis of the charge distribution and three-dimensional effects are required. Surface charging times and characteristic vehicle speeds were calculated under the assumption of a source current of 100 μA, representative of current electrospray thruster capabilities.

IV. Experimental Setup

The goal of the experiment was to demonstrate the feasibility of using ionic-liquid ion sources for combined vehicle and surface charging. Figure 6 shows a diagram of the test setup used in a vacuum chamber operated at pressures of around 10 μTorr and at room temperature. A test vehicle, wrapped in aluminum foil to distribute the charge over the surface and ensure constant potential, is suspended by two springs over an aluminum base plate. The setup is electrically insulated from the vacuum chamber walls by a teflon sheet. A tungsten rod is attached at the end of the springs

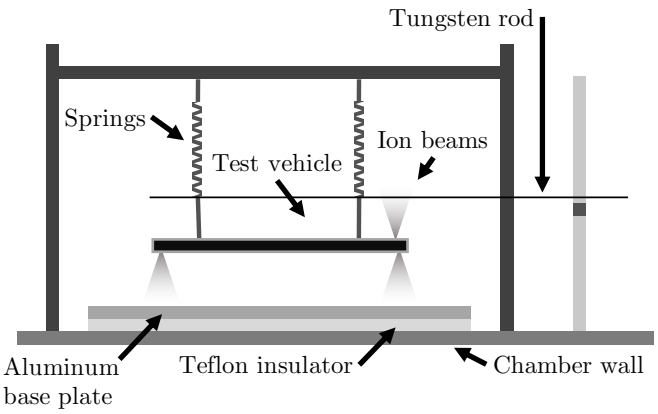

Fig. 6 Notional diagram of the test setup.

Table 3 Experimental setup parameters.

Parameter	Value
Test vehicle total mass	60 g
Test vehicle radius	75 mm
Test vehicle thickness	30 mm
Firing potential	1.9-2.4 kV
Emitted current	100-300 nA
Hovering height	10 mm
Equivalent spring constant	10 N/m
Deflection under gravitational load	59 mm

such that any vertical movement of the test vehicle due to external forces can be measured as a displacement of the tungsten rod relative to a marker. Relevant parameters from the experimental setup are summarized in Table 3.

The test vehicle is a hexagon of mass 60 g, average radius 7.5 cm, and thickness 3 cm and has five tungsten single-tip ionic-liquid ion sources. A model of the test vehicle, without aluminum foil wrapping, is shown in Figure 7. Four of the sources point downwards towards the aluminum base plate and can emit positive ions while the last source points upwards away from the base plate and can emit negative ions. For testing, single-tip sources were used as opposed to fully microfabricated electrospray thrusters in order to simplify the test setup. Single-tip sources have similar potential characteristics to electrospray thrusters so experimental results will be indicative

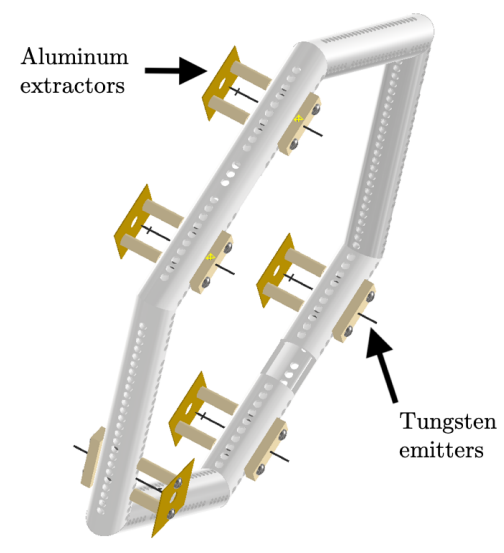

Fig. 7 Model of the test vehicle without aluminium foil wrapping.

of expected performance with full thrusters. For theoretical analyses, the shape of the test vehicle is approximated as a hollow disk of radius 7.5 cm and thickness 3 cm.

The ion sources were fabricated from tungsten wire according to Ref. [30] and used 1-Ethyl-3-methylimidazolium tetrafluoroborate as the ionic liquid. The source potential was provided by two PICO Electronics 5AV1500 high voltage DC-DC converters operated in series to allow source potentials from 0-3 kV and the current was measured through a 1±0.1 MΩ shunt resistor. As the actual source potential could not be measured during the experiment, the output of the converters at different input potentials was calibrated to within ±10 V prior to the experiment. The source potential could then be inferred based on the input potential to the high voltage converter. The input potential to the high-voltage converter was controlled with an LM317 voltage regulator to attenuate any noise and allow gradual application of the potential in order to avoid any droplet emission during the emission startup transient. Figure 8 shows the connections from the high-voltage converters into the vacuum chamber. Both the test vehicle and base plate are electrically isolated in order to allow their respective potentials to float in response to emitted current.

During experiments, the sources allowed a limited range of potentials to be tested. The lower limit of this range is given by the starting potential, which is approximated by

$$V_{\text{start}} = \sqrt{\frac{\gamma R_{\text{c}}}{\epsilon_0}} \ln\left(\frac{4l}{R_{\text{c}}}\right) \tag{27}$$

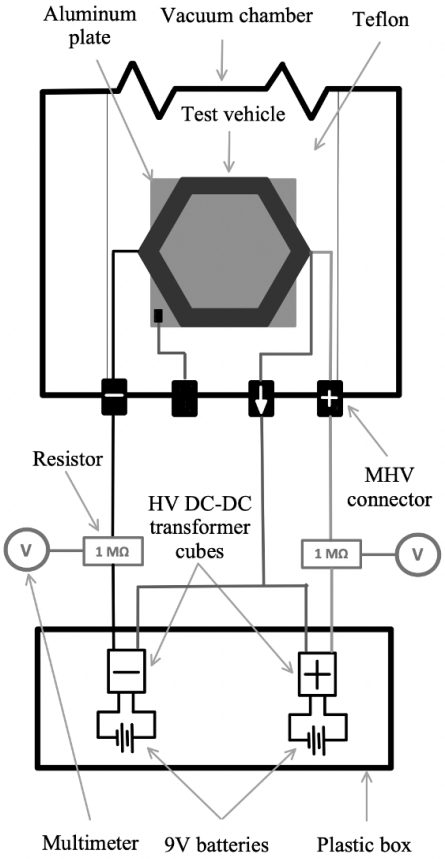

Fig. 8 Diagram of the electrical connections at the interface of the vacuum chamber.

where γ is the surface tension of the ionic liquid, R_c is the radius of curvature of the tungsten emitter tip, and l is the distance from the tip to the extractor grid [31]. For the ionic-liquid ion sources used in this work, the starting potential is approximately 1.9 kV, which was experimentally verified. The upper limit of the thruster potential range occurs at approximately 2.4 kV, where electrical shorts between the emitter tips and extractors started to be observed.

Given a test vehicle mass of 60 g and a thruster potential of 2 kV, Eq. 24 gives an expected levitation height of around 7×10^{-4} times the dimension of the test vehicle which corresponds to levitation heights on the order of 5 μm. This requires that the base of the test vehicle be suspended 5 μm above the base plate, severely constraining the test and measurement system. Therefore, the use of springs to offload the gravitational force is necessary to get clear measurements of the electrostatic force. Two springs, with spring constants of 5 N/m and each carrying half the weight, are used to balance the test vehicle's rotation and suspend it parallel to the base plate. The weight

of the test vehicle and expected electrostatic force are within the limits of the linear regime for the springs used during experiment.

The displacement of the tungsten rod was measured with a Dino-Lite 720p digital microscope with resolution and magnification such that each pixel corresponded to less than 1 μm of displacement. At this resolution, errors in determining the displacement of the tungsten rod due to pixel error will be two orders of magnitude lower than the expected displacement due to electrostatic force (of order 100 μm) and correspond to errors in the measured electrostatic force of 10 μN. In addition, measurements were taken at a frequency of 30 Hz. This value is much larger than the predicted 2 Hz natural frequency of the springs, which was experimentally verified to 10% margin of error. Therefore, equilibrium oscillations caused by disturbances due to external forces, such as the vibration of the vacuum pumps, should be captured and not cause a steady-state bias in the displacement measurement.

Figure 9 shows a diagram of the measurement process. With the thrusters off, the tungsten rod rests at an equilibrium displacement from the marker. When the ion sources facing the base plate are fired, the test vehicle and base plate charge to opposite polarities resulting in the test vehicle being attracted towards the base plate. The emitter firing away from the base plate can also be fired in order to charge the test vehicle and base plate to the same polarity, resulting in the test vehicle being repelled from the base plate. The displacement of the tungsten rod, d, is measured and related to the electrostatic force, F, through the spring constant, k, as

$$||F|| = kd \tag{28}$$

V. Experimental Results

Figure 10 shows an example of measured electrostatic force over time as a potential is applied to the emitters. In this particular example, a positive potential of 2.07 kV is first applied to the emitters pointed at the base plate. The resulting current charges the test vehicle negatively and the base plate positively resulting in the test vehicle being attracted to the base plate with an observed attractive force of approximately 0.96 mN. Next, the test vehicle is manually grounded before a negative potential of -1.8 kV is applied to the emitter pointed away from the base plate, charging

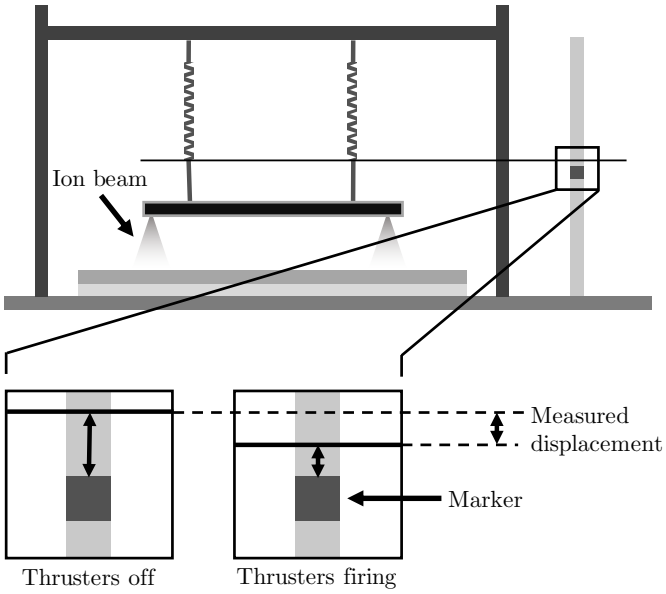

Fig. 9 Diagram of measurement of electrostatic force through deflection of the tungsten rod.

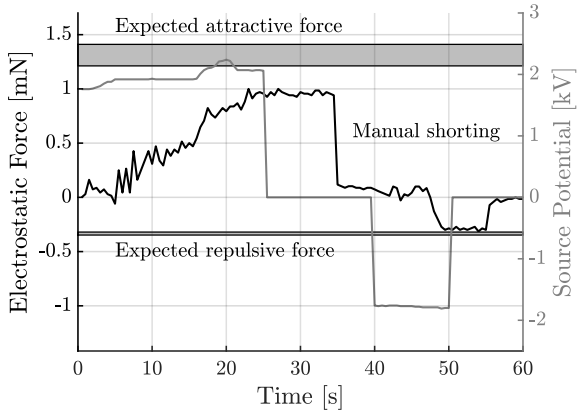

Fig. 10 Electrostatic force over time as potential is applied to the ion sources. Expected forces correspond to the expected force at the maximum source potential in each polarity and are shown as a region due to uncertainty in initial suspension height of the test vehicle.

the test vehicle positively. Since the base plate retains its positive charge, this results in the test vehicle being repelled away from the base plate with an observed repulsive force of approximately 0.29 mN. The electrostatic force appears to lag behind the applied source potential. This is due to a delay in the output current of the emitters relative to the application of the source potential and is an artifact of the experimental setup.

The shaded regions represent the expected electrostatic force based on Eqs. 13 and 14 and the

experimental parameters in Table 3 with the capacitance of the test vehicle estimated to be that of a finite disk with uniform charge distribution

$$C_{\mathrm{v}} = 2\pi\epsilon_0 r_{\mathrm{v}} \tag{29}$$

Due to the geometry of the test vehicle, the initial distance between the test vehicle and base plate is estimated to be 14-15 mm and causes uncertainty in the estimated force. Therefore, the expected force is shown as a region rather than as a single line. The prediction of the magnitude of the electrostatic force is greater than the observed force by approximately 0.35 mN for the attractive force (37% error) and 0.044 mN for the repulsive force (15% error). This is to be expected as several effects, such as the distribution of charge on the vehicle and secondary electron emission, were intentionally omitted from the theoretical model for simplicity. However, the low-order model is able to capture both the right magnitude of electrostatic force as well as the asymmetry between the attractive and repulsive forces.

Figure 11 shows the measured attractive electrostatic force as the source potential is varied along with the expected relationship from Eq. 13. The initial distance between the test vehicle and base plate is estimated to be 11-12 mm. Again, the model over-predicts the attractive force relative to the experimental data. This discrepancy could be due to further three-dimensional effects from the charge on the test vehicle being spread out over the vehicle's surface or the effect of secondary electrons. As ions return to the test vehicle, they can emit secondary electrons. If the test vehicle is charged negatively, as it is during the attractive force experiments, the secondary electrons can escape the vehicle and be attracted to the base plate, reducing the overall charge level of both the test vehicle and base plate and resulting in a corresponding decrease in the electrostatic force. Detailed analysis of the effects of secondary electron emission requires knowledge of the energy distribution of the emitted ions, which can vary significantly between different sources and propellants. However, a simple model that does not account for charge distribution or secondary electrons is still able to predict a magnitude of electrostatic force similar to the observed force, perhaps indicating that the influence of these effects is small.

Another potential source of error in the test setup is charge leakage to the environment either internal to the vacuum chamber or externally along the electronics connections. However, it is

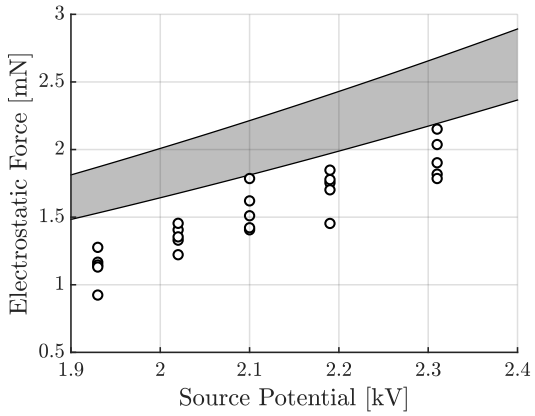

Fig. 11 Attractive electrostatic force versus source potential along with expected relationship based on low-order model. Expected relationship is shown as a region due to uncertainty in initial suspension height of the test vehicle.

believed that this effect is negligible. Figure 12 shows the average measured electrostatic force over time after the sources have been turned off for three different test runs. Error bars correspond to one standard deviation. The electrostatic force clearly drops over time which is indicative of charge, either on the test vehicle or base plate, leaking to the environment. Based on Figure 11, the reduction in electrostatic force over 60 s corresponds to a potential drop on the test vehicle of approximately 400 V. Given the estimated capacitance of the test vehicle, 4.2 pF, this corresponds to an average leakage current of 28 pA, well below the 100-300 nA of current provided by the ion sources. Incidentally, the ratio of source current to leakage current (100 nA/28 pA = 3571) is of the same order as the expected ratio of a full electrospray thruster current to plasma and photoelectron currents (150 μA/100 nA = 1500) allowing the leakage current observed during experiment to simulate the effects of plasma and photoelectron currents.

It is worth comparing the electrostatic force observed during this experiment to the use of propulsion systems in a traditional manner where reactive forces are generated through mass ejection in order to demonstrate the efficiency of the electrostatic concept. The electrostatic force in Figure 11 is approximately 1 mN and is generated through only around 100 nA of current. The mass of the cation of the ionic liquid 1-Ethyl-3-methylimidazolium tetrafluoroborate is 111.2 Da which gives a total mass flow during the experiments of approximately 1.2×10^{-10} g/s. Therefore, to produce

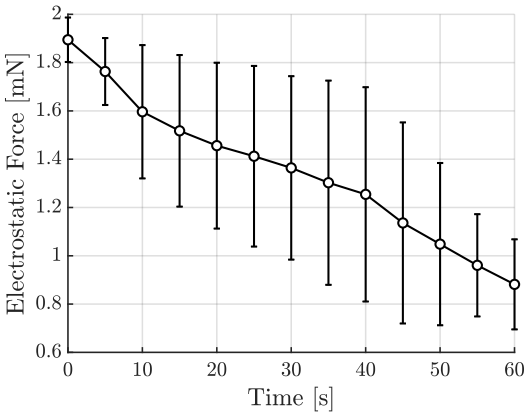

Fig. 12 Average measured electrostatic force over time after thrusters have been turned off demonstrating slow charge leakage. Error bars correspond to one standard deviation.

a force of 1 mN with the same mass flow, the propulsion system would need a specific impulse of approximately 8.7×10^8 s. Not only is this beyond the capabilities of current propulsion systems, but to operate a propulsion system at such a high specific impulse would require at least 4 MW of power whereas only 0.2 mW of power were required during this experiment to create the same force using electrostatic force through charge transport.

VI. Conclusion

The use of ionic-liquid ion sources for electrostatic levitation on atmosphere-less planetary bodies is analyzed and theoretical predictions on the relationship between electrostatic force and source potential are experimentally verified. A low-fidelity model predicts that levitation heights of approximately 0.1 the characteristic dimension of a 1 kg vehicle would be possible with a 10 kV ion source on a planetary body the size of Psyche and with a 50 kV ion source on a planetary body the size of the Moon, potentially enabling surface maneuverability. Experimental results confirm the qualitative predictions of the low-fidelity model and demonstrate that a 1 mN electrostatic force can be created through charge transport while only using 0.2 mW of input power.

A metallic base plate is used during experiments in order to allow the angular distribution of the ionic-liquid ion source plume to be ignored. The surfaces of many planetary bodies will be highly resistive and further experiments will be required to demonstrate similar performance with

insulating base plates. However, it is expected that performance should not differ significantly as the insulating surface will allow charge to more easily accumulate and the angular distribution of the source plume can be tuned in order to achieve a desired surface charge distribution. In addition, as the surface directly below the ion sources charges, it will cause the plume to spread and charge much of the surface below the vehicle.

The analytical model developed in this work is low fidelity and ignores effects such as the charge distribution of the vehicle and the surface, photoelectron and plasma current, and secondary electron emission. Of these effects, the distribution of charge is expected to be dominant. Both the photoelectron and plasma currents will be several orders of magnitude lower than the current produced by an ionic liquid ion source for a vehicle of the size considered here ($\sim$10 cm). The effects of secondary electron emission are also expected to be small as the positively charged surface will prevent them from escaping. Since the distribution of charge is unique to the vehicle, it cannot be considered here analytically but will be considered in future work.

Future work will also analyze the interaction of the ion beam with the surface of the planetary body. While the transfer of charge from the ion beam to the surface has been demonstrated here, it is unknown what other interactions there may be. It is possible that mass may be deposited on the surface, or that the ion beam will etch the top layer of the surface and have a cleaning effect. These effects are worth studying in order to ensure that there is not any potential contamination of the planetary body's surface due to irradiation with the ion beam.

Despite the low fidelity of the model, its close prediction ($\sim$30% error) of the experimental results provides confidence that electrostatic levitation with ionic liquid ion sources is a feasible concept. Electrostatic levitation aided by ion sources could be used to provide maneuverability for a spacecraft during proximity operations around a small asteroid as in Ref. [17] or to develop solid-state surface rovers that can traverse across a planetary body's surface with no moving parts. The prospect of a rover that can maneuver across a surface without any physical contact could allow for easier exploration of uneven surfaces relative to traditional wheeled and hopper robots. Wheeled mechanisms struggle with overly rough terrain which is abundant on planetary bodies in the form of rocks, craters, subterranean tunnels, and other steep terrain. These regions of rough terrain are

often also regions of scientific interest and the ability to access these areas could greatly increase the science return of future missions.

This work demonstrates, from an actuation standpoint, that such a rover could be possible with current technology. For planetary bodies with surface gravitation acceleration of 0.06 m/s^2 (representative of a planetary body the size of the asteroid Psyche), a 1 kg rover could levitate to heights several times its characteristic dimension with ion source potentials on the order of 25 kV. More detailed analysis of the limits on levitation height are required for cases where the flat-plate assumption for the local electric field breaks down or when plasma shielding becomes significant. In addition, design of both the altitude and attitude controllers for such a rover is required, particularly for cases where the terrain is not perpendicular to the local gravitational field.

In the case of spacecraft, particularly landers, the use of electrostatic levitation could be used to re-position the spacecraft after landing, broadening the potential area of the surface that the lander could analyze. In addition, the electrostatic force could serve to anchor the spacecraft to the surface of the planetary body. Current methods, such as the harpoon used in the Philae lander [32], require intricate mechanisms whose performance can depend on the material composition of the planetary body. The use of ionic-liquid ion sources, such as electrospray thrusters, could allow for a mechanically-simple anchoring system whose performance does not vary significantly with surface composition.

Funding Sources

Funding for this work was provided by the NASA Space Technology Mission Directorate through a NASA Space Technology Research Fellowship under grant 80NSSC18K1186. S. K. Hampl would like to thank the German Academic Scholarship Foundation for supporting his research stay at MIT. In addition, P. C. Lozano would like to thank the Miguel Alemán-Velasco Foundation for its support.

References

[1] Freeman, J. W. and Ibrahim, M., "Lunar Electric Fields, Surface Potential and Associated Plasma Sheaths," *The Moon*, Vol. 14, No. 1, 1975, pp. 103–114,

doi:10.1007/BF00562976.

[2] Halekas, J. S., Delory, G. T., Lin, R. P., Stubbs, T. J., and Farrell, W. M., "Lunar Prospector Observations of the Electrostatic Potential of the Lunar Surface and Its Response to Incident Currents," *Journal of Geophysical Research: Space Physics*, Vol. 113, Article 9, doi:10.1029/2008JA013194.

[3] Rennilson, J. J. and Criswell, D. R., "Surveyor Observations of Lunar Horizon-Glow," *The Moon*, Vol. 10, No. 2, 1974, pp. 121–142, doi:10.1007/BF00655715.

[4] Lee, P., "Dust Levitation on Asteroids," *Icarus*, Vol. 124, No. 1, 1996, pp. 181–194, doi:10.1006/icar.1996.0197.

[5] Hirata, N. and Miyamoto, H., "Dust Levitation as a Major Resurfacing Process on the Surface of a Saturnian Icy Satellite, Atlas," *Icarus*, Vol. 220, No. 1, 2012, pp. 106–113, doi:10.1016/j.icarus.2012.03.028.

[6] Robinson, M. S., Thomas, P. C., Veverka, J., Murchie, S., and Carcich, B., "The Nature of Ponded Deposits on Eros," *Nature*, Vol. 413, No. 6854, 2001, pp. 386–400, doi:10.1038/35096518.

[7] Murphy, T. W., Adelberger, E., Battat, J. B. R., Hoyle, C. D., McMillan, R. J., Michelsen, E. L., Samad, R. L., Stubbs, C. W., and Swanson, H. E., "Long-term Degradation of Optical Devices on the Moon," *Icarus*, Vol. 208, No. 1, 2010, pp. 31–35, doi:10.1016/j.icarus.2010.02.015.

[8] Vernazza, P., Delbo, M., King, P. L., Izawa, M. R. M., Olofsson, J., Lamy, P., Cipriani, F., Binzel, R. P., Marchis, F., Merín, B., and Tamanai, A., "High Surface Porosity as the Origin of Emissivity Features in Asteroid Spectra," *Icarus*, Vol. 221, No. 2, 2012, pp. 1162–1172, doi:10.1016/j.icarus.2012.04.003.

[9] Nordheim, T., Jones, G., Halekas, J., Roussos, E., and Coates, A., "Surface Charging and Electrostatic Dust Acceleration at the Nucleus of Comet 67P During Periods of Low Activity," *Planetary and Space Science*, Vol. 119, 2015, pp. 24–35, doi:10.1016/j.pss.2015.08.008.

[10] Thomas, N. et al., "Redistribution of Particles Across the Nucleus of Comet 67P/Churyumov-Gerasimenko," *Astronomy and Astrophysics*, Vol. 583, Article 17, doi:10.1051/0004-6361/201526049.

[11] Sheridan, T. E., Goree, J., Chiu, Y. T., Rairden, R. L., and Kiessling, J. A., "Observation of Dust

Shedding from Material Bodies in a Plasma," *Journal of Geophysical Research: Space Physics*, Vol. 97, Article 3,
doi:10.1029/91JA02801.

[12] Flanagan, T. M. and Goree, J., "Dust Release from Surfaces Exposed to Plasma," *Physics of Plasmas*, Vol. 13, No. 12, Paper 123504,
doi:10.1063/1.2401155.

[13] Wang, X., Horányi, M., and Robertson, S., "Investigation of Dust Transport on the Lunar Surface in a Laboratory Plasma with an Electron Beam," *Journal of Geophysical Research: Space Physics*, Vol. 115, Article 11,
doi:10.1029/2010JA015465.

[14] Wang, X., Colwell, J., Horanyi, M., and Robertson, S., "Charge of Dust on Surfaces in Plasma," *IEEE transactions on plasma science*, Vol. 35, No. 2, 2007, pp. 271–279,
doi:10.1109/TPS.2007.891639.

[15] Wang, X., Horányi, M., and Robertson, S., "Dust Transport Near Electron Beam Impact and Shadow Boundaries," *Planetary and Space Science*, Vol. 59, No. 14, 2011, pp. 1791–1794,
doi:10.1016/j.pss.2010.12.005.

[16] Wang, X., Schwan, J., Hsu, H. W., Grün, E., and Horányi, M., "Dust Charging and Transport on Airless Planetary Bodies," *Geophysical Research Letters*, Vol. 43, No. 12, 2016, pp. 6103–6110,
doi:10.1002/2016GL069491.

[17] Quadrelli, M. B., Garrett, H., Castillo, J., Stoica, A., Ono, M., Christianson, C., Lusso, D., and Schaub, H., "Active Electrostatic Flight for Airless Bodies," *Proceedings of the 38th IEEE Aerospace Conference*, Big Sky, MT, 2017,
doi:10.1109/AERO.2017.7943821.

[18] Deng, W., Klemic, J. F., Lee, X., Reed, M. A., and Gomez, A., "Increase of Electrospray Throughput Using Multiplexed Microfabricated Sources for the Scalable Generation of Monodisperse Droplets," *Journal of Aerosol Science*, Vol. 37, No. 6, 2006, pp. 696–714,
doi:10.1016/j.jaerosci.2005.05.011.

[19] Alexander, M. S., Stark, J., Smith, K. L., Stevens, B., and Kent, B., "Electrospray Performance of Microfabricated Colloid Thruster Arrays," *Journal of Propulsion and Power*, Vol. 22, No. 3, 2006, pp. 620–627,
doi:10.2514/1.15190.

[20] Legge, R. S. and Lozano, P. C., "Electrospray Propulsion Based on Emitters Microfabricated in Porous

Metals," *Journal of Propulsion and Power*, Vol. 27, No. 2, 2011, pp. 485–495, doi:10.2514/1.50037.

[21] Krejci, D., Mier-Hicks, F., Thomas, R., Haag, T., and Lozano, P. C., "Emission Characteristics of Passively Fed Electrospray Microthrusters with Propellant Reservoirs," *Journal of Spacecraft and Rockets*, Vol. 54, No. 2, 2017, pp. 447–458, doi:10.2514/1.A33531.

[22] Mier-Hicks, F. and Lozano, P. C., "Spacecraft-Charging Characteristics Induced by the Operation of Electrospray Thrusters," *Journal of Propulsion and Power*, Vol. 33, No. 2, 2017, pp. 456–467, doi:10.2514/1.B36292.

[23] Miller, C. E., *Characterization of Ion Cluster Fragmentation in Ionic Liquid Ion Sources*, Ph.D. thesis, Massachusetts Institute of Technology, 2019.

[24] Whipple, E. C., "Potentials of Surfaces in Space," *Reports on Progress in Physics*, Vol. 44, No. 11, 1981, pp. 1197–1250, doi:10.1088/0034-4885/44/11/002.

[25] Halekas, J. S., Lin, R. P., and Mitchell, D. L., "Large Negative Lunar Surface Potentials in Sunlight and Shadow," *Geophysical Research Letters*, Vol. 32, 2005, p. L09102, doi:10.1029/2005GL022627.

[26] Mommert, M. et al., "Physical Properties of Near-Earth Asteroid 2011 MD," *The Astrophysical Journal Letters*, Vol. 789, No. 1, doi:10.1088/2041-8205/789/1/L22.

[27] Pravec, P., Hergenrother, C., Whiteley, R., ÅăarounovÃą, L., KuÅąnirÃąk, P., and Wolf, M., "Fast Rotating Asteroids 1999 TY2, 1999 SF10, and 1998 WB2," *Icarus*, Vol. 147, No. 2, 2000, pp. 477–486, doi:10.1006/icar.2000.6458.

[28] Morea, S. F., "The Lunar Roving Vehicle - Historical Perspective," *Proceedings of the 2nd Conference on Lunar Bases and Space Activities*, Houston, TX, 1992.

[29] Malenkov, M., "Self-Propelled Automatic Chassis of Lunokhood-1: History of Creation in Episodes," *Frontiers of Mechanical Engineering*, Vol. 11, No. 1, , pp. 60–86, doi:10.1007/s11465-016-0370-5.

[30] Lozano, P. C. and MartÃŋnez-SÃąnchez, M., "Ionic Liquid Ion Sources: Characterization of Externally Wetted Emitters," *Journal of Colloid and Interface Science*, Vol. 282, No. 2, 2005, pp. 415–421, doi:10.1016/j.jcis.2004.08.132.

[31] Hruby, V., Gamero-Castaño, M., Cordero, J., Kolencik, J., and Martínez-Sánchez, M., "Colloid

Thrusters for Micro and Nano-Satellites," , 1999. Final report, Phase I SBIR NASA.

[32] Ulamec, S. and Biele, J., "Surface Elements and Landing Strategies for Small Bodies Missions–Philae and Beyond," *Advances in Space Research*, Vol. 44, No. 7, 2009, pp. 847–858, doi:10.1016/j.asr.2009.06.009.